

Relativistic many-body calculations of excitation energies and transition rates in ytterbium-like ions

U. I. Safronova,* W. R. Johnson,† and M. S. Safronova‡
Department of Physics, 225 Nieuwland Science Hall
University of Notre Dame, Notre Dame, IN 46566

J. R. Albritton
Lawrence Livermore National Laboratory, PO Box 808, Livermore, CA 94551
(Dated: October 24, 2018)

Excitation energies, oscillator strengths, and transition rates are calculated for $(5d^2 + 5d6s + 6s^2) - (5d6p + 5d5f + 6s6p)$ electric dipole transitions in Yb-like ions with nuclear charges Z ranging from 72 to 100. Relativistic many-body perturbation theory (RMBPT), including the retarded Breit interaction, is used to evaluate retarded E1 matrix elements in length and velocity forms. The calculations start from a $[\text{Xe}]4f^{14}$ core Dirac-Fock potential. First-order RMBPT is used to obtain intermediate coupling coefficients, and second-order RMBPT is used to determine matrix elements. A detailed discussion of the various contributions to energy levels and dipole matrix elements is given for ytterbium like rhenium, $Z=75$. The resulting transition energies are compared with experimental values and with results from other recent calculations. Trends of excitation energies, line strengths, oscillator strengths, and transition rates as functions of nuclear charge Z are shown graphically for selected states and transitions. These calculations are presented as a theoretical benchmark for comparison with experiment and theory.

PACS numbers: PACS: 32.70.Cs, 31.15.Md, 31.25.Eb, 31.25.Jf, 31.30.Jv

I. INTRODUCTION

We report results of *ab initio* calculations of excitation energies, oscillator strengths, and transition rates in Yb-like ions with nuclear charges Z ranging from 72 to 100. The ions considered here, starting from doubly ionized Hf III, all have $5d^2$ ground states. We do not consider Yb I and Lu II both of which have a $6s^2$ ground state configuration. In recent publications [1, 2, 3, 4, 5, 6, 7], the spectra of Re VI, Os VII, and Ir VIII were studied and energies levels of the $5d^2$, $5d6s$, $5d6p$, $5d5f$ and $6s6p$ configurations were determined. The Cowan Hartree-Fock code [8] with relativistic and correlation options was used in Refs. [1, 2, 3, 4, 5, 6, 7] to calculate energy levels and to carry out least-squares adjustments of energies.

Although we do not consider Yb I and Lu II here, it should be noted that Porsev et al. [9] recently carried out elaborate calculations of electric-dipole amplitudes in atomic ytterbium. Moreover, Martin et al. [10] listed energies for 249 levels of Yb I and 40 levels of Lu II.

In the present paper, we use relativistic many-body perturbation theory (RMBPT) to determine energies of the 14 even-parity $5d^2$, $5d6s$, and $6s^2$ states and the 36 odd-parity $5d6p$, $5d5f$, and $6s6p$ states for Yb-like ions. We illustrate our calculation with a detailed study of Re VI, $Z=75$. Our first-order RMBPT calculations

include both the Coulomb and retarded Breit interactions but our second-order calculations are limited to the Coulomb interaction only.

Reduced matrix elements, line strengths, oscillator strengths, and transition rates are determined for all allowed and forbidden electric-dipole transitions between even-parity ($5d^2 + 5d6s + 6s^2$) and odd-parity ($5d6p + 5d5f + 6s6p$) states. Retarded E1 matrix elements are evaluated in both length and velocity forms. RMBPT calculations that start from a local potential are gauge independent order-by-order, provided “derivative terms” are included in second- and higher-order matrix elements and careful attention is paid to negative-energy states. The present calculations start from a nonlocal $[\text{Xe}]4f^{14}$ Dirac-Fock (DF) potential and consequently give gauge-dependent transition matrix elements. Second-order correlation corrections compensate almost exactly for the gauge dependence of the first-order matrix elements and lead to corrected matrix elements that differ by less than 5% in length and velocity forms for all of the ions considered here.

Energies from the present calculation agree well with results given in Refs. [1, 2, 3, 4, 5, 6, 7] for low-lying levels, but disagree substantially for various highly-excited levels, as discussed later.

II. METHOD

The RMBPT formalism developed previously [11, 12, 13, 14, 15] for Be-, Mg-, and Ca-like ions is used here to describe perturbed wave functions, to obtain the second-order energies [11], and to evaluate first- and second-

*Electronic address: usafrono@nd.edu

†Electronic address: johnson@nd.edu; URL: www.nd.edu/~johnson

‡Electronic address: msafrono@nd.edu; Current address: Electron and Optical Physics Division, National Institute of Standards and Technology, Gaithersburg, MD, 20899-8410

TABLE I: Possible two-particle states in the Yb-like ions

jj coupling	LS coupling	jj coupling	LS coupling
$5d_{3/2}5d_{3/2}(0)$	$5d^2 \ ^3P_0$	$5d_{3/2}6p_{1/2}(2)$	$5d6p \ ^3F_2$
$5d_{5/2}5d_{5/2}(0)$	$5d^2 \ ^1S_0$	$5d_{3/2}6p_{3/2}(2)$	$5d6p \ ^3D_2$
$6s_{1/2}6s_{1/2}(0)$	$6s^2 \ ^1S_0$	$5d_{5/2}6p_{1/2}(2)$	$5d6p \ ^1D_2$
		$5d_{5/2}6p_{3/2}(2)$	$5d6p \ ^3P_2$
$5d_{3/2}5d_{5/2}(1)$	$5d^2 \ ^3P_1$	$5d_{3/2}5f_{5/2}(2)$	$6s6p \ ^3P_2$
$5d_{3/2}6s_{1/2}(1)$	$5d6s \ ^3D_1$	$5d_{3/2}5f_{7/2}(2)$	$5d5f \ ^3F_2$
		$5d_{5/2}5f_{5/2}(2)$	$5d5f \ ^1D_2$
$5d_{3/2}5d_{3/2}(2)$	$5d^2 \ ^3F_2$	$5d_{5/2}5f_{7/2}(2)$	$5d5f \ ^3D_2$
$5d_{3/2}5d_{5/2}(2)$	$5d^2 \ ^1D_2$	$6s_{1/2}6p_{3/2}(2)$	$5d5f \ ^3P_2$
$5d_{5/2}5d_{5/2}(2)$	$5d^2 \ ^3P_2$		
$5d_{3/2}6s_{1/2}(2)$	$5d6s \ ^3D_2$	$5d_{3/2}6p_{3/2}(3)$	$5d6p \ ^3F_3$
$5d_{5/2}6s_{1/2}(2)$	$5d6s \ ^1D_2$	$5d_{5/2}6p_{1/2}(3)$	$5d6p \ ^3D_3$
		$5d_{5/2}6p_{3/2}(3)$	$5d6p \ ^1F_3$
$5d_{3/2}5d_{5/2}(3)$	$5d^2 \ ^3F_3$	$5d_{3/2}5f_{5/2}(3)$	$5d5f \ ^3F_3$
$5d_{5/2}6s_{1/2}(3)$	$5d6s \ ^3D_3$	$5d_{3/2}5f_{7/2}(3)$	$5d5f \ ^3G_3$
		$5d_{5/2}5f_{5/2}(3)$	$5d5f \ ^3D_3$
$5d_{3/2}5d_{5/2}(4)$	$5d^2 \ ^3F_4$	$5d_{5/2}5f_{7/2}(3)$	$5d5f \ ^1F_3$
$5d_{5/2}5d_{5/2}(4)$	$5d^2 \ ^1G_4$		
		$5d_{5/2}6p_{3/2}(4)$	$5d6p \ ^3F_4$
$5d_{3/2}6p_{3/2}(0)$	$5d6p \ ^3P_0$	$5d_{3/2}5f_{5/2}(4)$	$5d5f \ ^1G_4$
$5d_{5/2}5f_{5/2}(0)$	$6s6p \ ^3P_0$	$5d_{3/2}5f_{7/2}(4)$	$5d5f \ ^3H_4$
$6s_{1/2}6p_{1/2}(0)$	$5d5f \ ^3P_0$	$5d_{5/2}5f_{5/2}(4)$	$5d5f \ ^3F_4$
		$5d_{5/2}5f_{7/2}(4)$	$5d5f \ ^3G_4$
$5d_{3/2}6p_{1/2}(1)$	$5d6p \ ^3D_1$		
$5d_{3/2}6p_{3/2}(1)$	$5d6p \ ^3P_1$	$5d_{3/2}5f_{7/2}(5)$	$5d5f \ ^3H_5$
$5d_{5/2}6p_{3/2}(1)$	$5d6p \ ^1P_1$	$5d_{5/2}5f_{5/2}(5)$	$5d5f \ ^3G_5$
$5d_{3/2}5f_{5/2}(1)$	$6s6p \ ^3P_1$	$5d_{5/2}5f_{7/2}(5)$	$5d5f \ ^1H_5$
$5d_{5/2}5f_{5/2}(1)$	$5d5f \ ^3D_1$		
$5d_{5/2}5f_{7/2}(1)$	$6s6p \ ^1P_1$	$5d_{5/2}5f_{7/2}(6)$	$5d5f \ ^3H_6$
$6s_{1/2}6p_{1/2}(1)$	$5d5f \ ^3P_1$		
$6s_{1/2}6p_{3/2}(1)$	$5d5f \ ^1P_1$		

TABLE II: Contributions to energy matrices $E[Q, Q']$ (a.u.) for odd-parity states $Q=n_1l_1j_1n_2l_2j_2(J)$, $Q'=n_3l_3j_3n_4l_4j_4(J)$ with $J=0$ before diagonalization in the case of Yb-like rhenium, $Z = 75$.

Q, Q'	$E^{(0)}$	$E^{(1)}$	$B^{(1)}$	$E^{(2)}$
$5d_{3/2}6p_{3/2}, 5d_{3/2}6p_{3/2}$	-3.99398	0.42731	0.00679	-0.14018
$5d_{5/2}5f_{5/2}, 5d_{5/2}5f_{5/2}$	-3.42978	0.44889	0.00430	-0.16664
$6s_{1/2}6p_{1/2}, 6s_{1/2}6p_{1/2}$	-3.64181	0.29737	0.00591	-0.10004
$5d_{3/2}6p_{3/2}, 5d_{5/2}5f_{5/2}$		-0.01871	0.00003	0.01465
$5d_{5/2}5f_{5/2}, 5d_{3/2}6p_{3/2}$		-0.01871	0.00003	0.00965
$5d_{3/2}6p_{3/2}, 6s_{1/2}6p_{1/2}$		0.02191	-0.00001	-0.01278
$6s_{1/2}6p_{1/2}, 5d_{3/2}6p_{3/2}$		0.02191	-0.00001	-0.00996
$5d_{5/2}5f_{5/2}, 6s_{1/2}6p_{1/2}$		-0.01992	-0.00001	0.00221
$6s_{1/2}6p_{1/2}, 5d_{5/2}5f_{5/2}$		-0.01992	-0.00001	0.00252

order transition matrix elements [13]. Ions of the Yb sequence, starting from the Hf III ion [16] and continuing onward have a $5d^2$ ground state. This is similar to the previously studied Ca sequence [15], where ions starting from Ti III have a $3d^2$ ground state. The primary differences between calculations for Ca-like and Yb-like ions arise from the increased number of the orbitals in the DF core potential, [Xe] $4f^{14}$ instead of [Ar] ([Ar] =

$1s^22s^22p^63s^23p^6$ and [Xe] = [Ar] $3d^{10}4s^24p^64d^{10}5s^25p^6$), and the strong mixing between both even-parity ($5d^2 + 5d6s + 6s^2$) and odd-parity ($5d6p + 5d5f + 6s6p$) states. These differences lead to much more laborious numerical calculations. The calculations are carried out using sets of DF basis orbitals that are linear combinations of B-splines. These B-spline basis orbitals are determined using the method described in Ref. [17]. We use 40 B-splines of order 8 for each single-particle angular momentum state and we include all orbitals with orbital angular momentum $l \leq 7$ in our basis set.

A. Model space

The model spaces for the ($5d^2 + 5d6s + 6s^2$) and ($5d6p + 5d5f + 6s6p$) complexes in Yb-like ions have 14 even-parity states and 36 odd-parity states, respectively. These states are summarized in Table I, where both jj and LS designations are given. When starting calculations from DF wave functions, it is natural to use jj designations for uncoupled matrix elements; however, neither jj - nor LS -coupling describes *physical* states properly, except for the single-configuration state $5d_{5/2}5f_{7/2}(6) \equiv 5d5f \ ^3H_6$. The strong mixing between $5d6p$, $5d5f$, and $6s6p$ states was discussed previously in Refs. [1, 2, 3, 4, 5, 6, 7].

B. Example: energy matrix for Re^{+5}

Details of the theoretical method used to evaluate second-order energies for ions with two valence electrons are given in Refs. [11, 12] and will not be repeated here. The energy calculations are illustrated in Table II, where we list contributions to the energies of odd-parity $J = 0$ states of Re^{+5} . We present zeroth-, first-, and second-order Coulomb energies $E^{(0)}$, $E^{(1)}$, and $E^{(2)}$ together with the first-order retarded Breit corrections $B^{(1)}$ [18]. It should be mentioned that the difference between first-order Breit corrections calculated with and without retardation is less than 2%. As one can see from Table II, the ratio of off-diagonal to diagonal matrix elements is larger for second-order contributions than for first-order contributions. Another difference between first- and second-order contributions concerns symmetry properties: first-order off-diagonal matrix elements are symmetric, whereas second-order off-diagonal matrix elements are unsymmetric (Lindgren and Morrison [19, chap. 9]). Indeed, $E^{(2)}[Q, Q']$ and $E^{(2)}[Q', Q]$ differ in some cases by 20-50% and occasionally even have opposite signs. The ratio of off-diagonal to diagonal matrix elements for Breit corrections $B^{(1)}$ is much smaller than for Coulomb corrections.

After evaluating the energy matrices, we calculate eigenvalues and eigenvectors for states with given values of J and parity. There are two possible methods to carry out the diagonalization: either diagonalize the

TABLE III: Energy of $5d^2$, $5d6s$, $6s^2$, $5d6p$, $5d5f$, and $6s6p$ states in Yb-like Re^{+5} (cm^{-1}). Notation: $E^{(0+1)} = E^{(0)} + E^{(1)} + B^{(1)}$.

Level	$E^{(0+1)}$			$E^{(2)}$			$E^{(\text{exc})}$
	Absolute energies			Excitation energies			
$5d^2 \ ^3F_2$	-1184024	-40817	-1224841	0	0	0	0
$5d^2 \ ^3F_3$	-1177178	-39172	-1216350	6847	1645	8491	
$5d^2 \ ^3F_4$	-1170966	-38780	-1209746	13058	2037	15095	
$5d^2 \ ^3P_0$	-1167037	-43309	-1210346	16987	-2493	14495	
$5d^2 \ ^1D_2$	-1166402	-41572	-1207975	17622	-756	16866	
$5d^2 \ ^3P_1$	-1163473	-41812	-1205285	20551	-995	19556	
$5d^2 \ ^3P_2$	-1156318	-40152	-1196470	27706	665	28371	
$5d^2 \ ^1G_4$	-1155966	-42068	-1198034	28059	-1251	26807	
$5d^2 \ ^1S_0$	-1127568	-46217	-1173785	56456	-5400	51056	
$5d6s \ ^3D_1$	-1097044	-35141	-1132185	86980	5675	92656	
$5d6s \ ^3D_2$	-1094845	-35442	-1130287	89180	5375	94554	
$5d6s \ ^3D_3$	-1087729	-33669	-1121397	96296	7148	103444	
$5d6s \ ^1D_2$	-1079142	-36325	-1115467	104883	4491	109374	
$5d6p \ ^3F_2$	-1030357	-30866	-1061223	153667	9951	163618	
$5d6p \ ^3D_1$	-1024847	-33457	-1058303	159178	7360	166538	
$5d6p \ ^3D_2$	-1018155	-30518	-1048673	165869	10299	176168	
$5d6p \ ^3F_3$	-1017295	-30334	-1047629	166729	10483	177212	
$5d6p \ ^1D_2$	-1012677	-29311	-1041988	171347	11505	182853	
$5d6p \ ^3D_3$	-1007838	-30332	-1038169	176187	10485	186672	
$5d6p \ ^3P_1$	-1005870	-31934	-1037804	178154	8882	187037	
$5d6p \ ^3P_0$	-1004380	-31262	-1035642	179644	9554	189199	
$5d6p \ ^3F_4$	-1001386	-28009	-1029395	182639	12807	195446	
$5d6p \ ^3P_2$	-999246	-29109	-1028355	184778	11708	196486	
$5d6p \ ^1F_3$	-995855	-31244	-1027099	188169	9573	197742	
$6s^2 \ ^1S_0$	-991963	-34225	-1026189	192061	6592	198652	
$5d6p \ ^3P_1$	-989455	-34880	-1024335	194569	5936	200506	
$6s6p \ ^3P_0$	-941422	-21782	-963204	242603	19035	261637	
$6s6p \ ^3P_1$	-936597	-22693	-959291	247427	18123	265550	
$6s6p \ ^3P_2$	-921614	-21582	-943197	262410	19234	281644	
$5d5f \ ^1G_4$	-914890	-27340	-942229	269135	13477	282611	
$5d5f \ ^3H_4$	-911078	-28960	-940038	272946	11857	284803	
$5d5f \ ^3H_5$	-910564	-26917	-937481	273460	13900	287360	
$5d5f \ ^3F_2$	-909842	-32013	-941855	274182	8804	282986	
$5d5f \ ^3F_3$	-907828	-33638	-941466	276197	7178	283375	
$5d5f \ ^3H_6$	-905206	-23491	-928698	278818	17325	296143	
$5d5f \ ^3F_4$	-903304	-28769	-932074	280720	12047	292767	
$5d5f \ ^1D_2$	-900678	-34598	-935275	283347	6219	289565	
$5d5f \ ^3D_1$	-898884	-36856	-935740	285140	3960	289100	
$5d5f \ ^3G_3$	-897436	-41168	-938604	286588	-352	286237	
$5d5f \ ^3D_2$	-893563	-36014	-929576	290462	4803	295265	
$6s6p \ ^1P_1$	-892813	-36571	-929383	291211	4246	295457	
$5d5f \ ^3G_4$	-892131	-38708	-930839	291893	2108	294002	
$5d5f \ ^3D_3$	-891083	-38081	-929165	292941	2735	295676	
$5d5f \ ^3G_5$	-889833	-39291	-929124	294191	1526	295717	
$5d5f \ ^3P_2$	-887212	-36551	-923763	296812	4266	301078	
$5d5f \ ^3P_1$	-886406	-36865	-923271	297619	3952	301570	
$5d5f \ ^3P_0$	-886124	-36385	-922510	297900	4431	302331	
$5d5f \ ^1F_3$	-884984	-39786	-924770	299040	1031	300071	
$5d5f \ ^1H_5$	-872058	-49224	-921282	311966	-8407	303559	
$5d5f \ ^1P_1$	-866971	-40448	-907419	317054	369	317422	

sum of zeroth- and first-order matrices, then calculate the second-order contributions using the resulting eigenvectors; or diagonalize the sum of the zeroth-, first- and second-order matrices together. Following Ref. [12], we choose the second method here.

The energy calculations are illustrated for Re^{+5} in Table III. Energies listed under the heading ‘‘Absolute energies’’ are given relative to the $[\text{Xe}]4f^{14}$ core, while those listed under the heading ‘‘Excitation energies’’ are given relative to the $5d^2 \ ^3F_2$ ground state. In the table, we present absolute zeroth- plus first-order Coulomb and Breit energies $E^{(0+1)} = E^{(0)} + E^{(1)} + B^{(1)}$, absolute second-order Coulomb energies $E^{(2)}$, and the sum $E^{(\text{tot})}$. We also give the breakdown excitation energies and total excitation energies $E^{(\text{exc})}$. As can be seen from the table, the second-order contribution is about 3% of the absolute energy but accounts for 5% – 15% of the excitation energy. This table clearly illustrates the importance of including second-order contributions. As mentioned previously, neither jj - nor LS -coupling describes physical states properly; nevertheless, we use LS designations to label levels. We organize levels in the table according to decreasing values of $E^{(0+1)}$. After including second-order corrections, the present ordering differs in some cases from the ordering according to decreasing $E^{(\text{tot})}$. Thus, the ordering of $5d^2 \ ^3F_4$ and $5d^2 \ ^3P_0$ levels, $5d5f \ ^3H_5$ and $5d5f \ ^3F_2$ levels, and $5d5f \ ^3G_4$ and $6s6p \ ^1P_1$ levels are interchanged in Re^{+5} after second-order corrections are added.

Problems arising when using different model spaces in RMBPT theory were examined by Johnson et al. [12]. A major difference between Yb-like and Be-like systems, is that we could not construct as complete a model space for a two-electron system with a $[\text{Xe}]4f^{14}$ core as we did for a system with a $[\text{He}]$ core [11]. To do so would require us to include all possible two-particle states that could be constructed from unoccupied $n=5$ and $n=6$ orbitals in our model space. In the case of Be-like ions, the model space is much simpler, being constructed from $n=2$ orbitals only. A second, but related, problem is that different model spaces lead to different results. For example, energy levels of Hg I, calculated using RMBPT with $(6s6p)$ and $(6s^2 + 6p^2)$ model spaces differed from those calculated with $(6s6p+6p6d)$ and $(6s^2+6p^2+6s6d)$ model spaces by about 500 cm^{-1} [12]. We confirm this result here comparing calculations of $5p6d$ energy levels starting from a $5p6d$ model space and those starting from $(5p6d + 5d5f)$ or $(5p6d + 5d5f + 6s6p)$ model spaces in Re^{+5} . The largest difference occurs in the $E^{(2)}$, which changes by 1000 cm^{-1} in some cases. The change in $E^{(0+1)}$ is smaller by a factor of two and has an opposite sign. The resulting change in $E^{(\text{tot})}$ is about 500 cm^{-1} . Similar tests of model-space dependence along the Yb sequence set a limit of about 500 cm^{-1} on the accuracy of the present second-order calculations.

C. Z -dependence of energies

One unique feature of the present calculations is the inclusion of second-order correlation corrections. We illustrate the Z -dependence of the second-order energy $E^{(2)}$ in Fig. 1 for even-parity levels with $J=2$ ($5d^2\ ^3F_2, ^1D_2, ^3P_2$ and $5d6s\ ^1, ^3D_2$) and $J=3, 4$ ($5d^2\ ^3F_3, ^3F_4, ^1G_4$ and $5d6s\ ^3D_3$). As can be seen from this figure, the second-order energy, $E^{(2)}$ slowly increases with Z in the range $3\text{--}5\times 10^4\ \text{cm}^{-1}$. The smooth Z -dependence for these nine terms is exceptional and is not found for other terms discussed below.

Excitation energies $E^{(\text{exc})}$ of even-parity and odd-parity states relative to the $5d^2\ ^3F_2$ ground state, divided by $(Z - 65)^2$, are shown in Figs. 2 and 3. Both designations are shown in these figures: LS for low Z and jj for high Z . The variation of the $5d^2$ levels with Z shown in Fig. 2a. Strong mixing between $5d_{3/2}5d_{5/2}(J)$ and $5d_{5/2}5d_{5/2}(J)$ states with $J=2$ or 4 leads to rapid variations with Z in the corresponding Grotrian diagrams. Note that the 1D_2 and 3F_4 levels cross between $Z=79$ and 80, 3P_0 and 3F_3 levels cross between $Z=80$ and 81, and 3P_1 and 3F_4 levels cross between $Z=93$ and 94. We give excitation energies of the other five even-parity $5d6s$ and $6s^2$ levels in Fig. 2b. Two small sharp features in the $6s^2$ level occur at $Z=82$ and $Z=85$. The origin of these irregularities is discussed in Appendix A. Energies of odd-parity levels with $J=0$ and 4, including mixing of $5d6p$, $5d5f$ and $6s6p$ states, are given in Fig. 3. The sharp features in the curves describing $5d5f$ and $6s6p$ states are similar to those mentioned above for even-parity states and discussed in Appendix A. Avoided level crossings for the odd-parity $J = 0$ levels are seen Fig. 3a near $Z=76$ and $Z=84$. Similar avoided crossings can be observed for the odd-parity complex with $J=4$ in Fig. 3b.

D. Z -dependence of matrix elements for electric-dipole transitions

We designate the first-order dipole matrix element by $Z^{(1)}$, the Coulomb correction to the second-order matrix element by $Z^{(2)}$, and the second-order Breit correction by $B^{(2)}$. The evaluation of $Z^{(1)}$, $Z^{(2)}$, and $B^{(2)}$ for Yb-like ions follows the pattern of the corresponding calculation for beryllium-like ions in Refs. [13, 20]. These matrix elements are calculated in both length and velocity gauges. Differences between length and velocity forms, are illustrated for the uncoupled $5d_{3/2}5d_{5/2}(2)\text{--}5d_{5/2}6p_{1/2}(3)$ matrix element in Fig. 4. The second-order Breit matrix element $B^{(2)}$ is multiplied by a factor of 50 in order to put it on the same scale as the second-order Coulomb matrix element $Z^{(2)}$. The sharp features have the same origin as those in the the second-order energy matrix and are discussed in Appendix B. Contributions of the second-order matrix elements $Z^{(2)}$ and $B^{(2)}$ are much larger in velocity (V) form than in length (L) form as seen in panels (a) and (b) of Fig. 4. As shown later, $L\text{--}V$ differences are

compensated by “derivative terms” $P^{(\text{deriv})}$.

E. Example: dipole matrix elements in Re^{+5}

We list uncoupled first- and second-order dipole matrix elements $Z^{(1)}$, $Z^{(2)}$, $B^{(2)}$, together with derivative terms $P^{(\text{deriv})}$ for Re^{+5} in Table IV. For simplicity, we consider only the 9 dipole transitions between even-parity states with $J=0$ and odd-parity states with $J=1$. The derivative terms shown in Table IV arise because transition amplitudes depend on energy, and the transition energy changes order-by-order in perturbation theory. Both L and V forms are given for the matrix elements. We see that the first-order matrix elements $Z_L^{(1)}$ and $Z_V^{(1)}$ differ by 10-20% and that the $L\text{--}V$ differences between second-order matrix elements are much larger for some transitions. The first-order matrix elements $Z_L^{(1)}$ and $Z_V^{(1)}$ are non-zero for the three matrix elements $5d_{3/2}5d_{3/2}(0)\text{--}5d_{3/2}6p_{1/2}(1)$, $5d_{3/2}5d_{3/2}(0)\text{--}5d_{3/2}6p_{3/2}(1)$, and $5d_{5/2}5d_{5/2}(0)\text{--}5d_{5/2}6p_{3/2}(1)$, but vanish for the remaining six transitions. Moreover, those six transitions, $Z_L^{(2)}$ and $Z_V^{(2)}$ have the same order of magnitude as the three non-zero first-order matrix elements. This confirms the importance of including higher-order RMBPT corrections. It can also be seen from Table IV that $P_L^{(\text{deriv})}$ is almost equal to $Z_L^{(1)}$ but $P_V^{(\text{deriv})}$ is smaller than $Z_V^{(1)}$ by five to six orders of magnitude.

In Table V, line strengths for Re^{+5} in length and velocity forms are given for the $J=0\text{--}J'=1$ transitions considered in Table IV as well as for other $J\text{--}J'$ transitions. We see that L and V forms of the coupled matrix elements in Table V differ only in the second or third digits. As mentioned in the introduction, these $L\text{--}V$ differences arise because we start our RMBPT calculations using a non-local DF potential. If we were to replace the DF potential by a local potential, the differences would disappear completely. Another source of $L\text{--}V$ differences is the use of an incomplete model space. The last two columns in Table V show L and V values of line strengths calculated without the second-order contribution. As can be seen, including second-order corrections significantly decreases $L\text{--}V$ differences.

III. RESULTS AND DISCUSSION

We calculate energies of the 14 even-parity $5d^2$, $5d6s$, and $6s^2$ states as well as the 36 odd-parity $5d6p$, $5d5f$, and $6s6p$ states for Yb-like ions with nuclear charges in the range $Z = 72$ to 100. Reduced matrix elements, line strengths, oscillator strengths, and transition rates are also determined for all electric-dipole transitions between even-parity and odd-parity states for each ion. Comparisons with experimental data and other theoretical results are also given. Our results are presented in three parts: transition energies, fine-structure energy differences, and

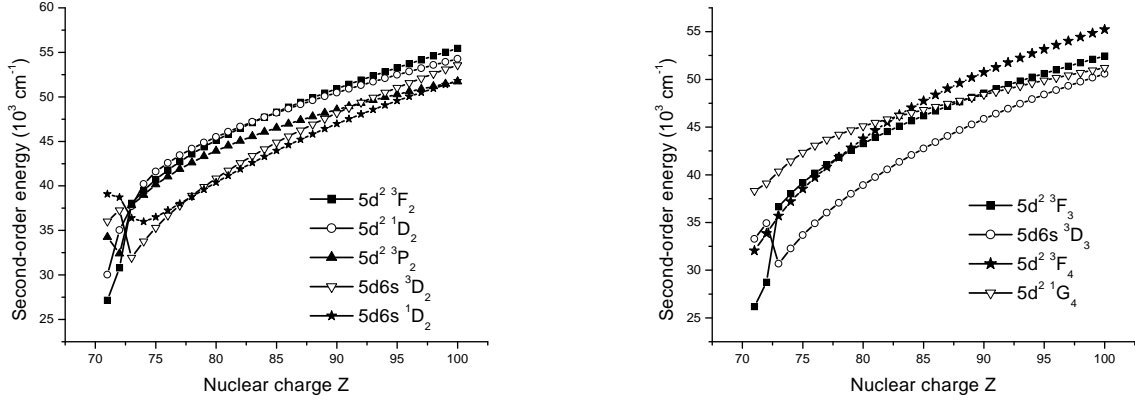


FIG. 1: Z -dependence of the second-order energy $E^{(2)}$ for the $5d^2$ and $5d6s$ energy levels

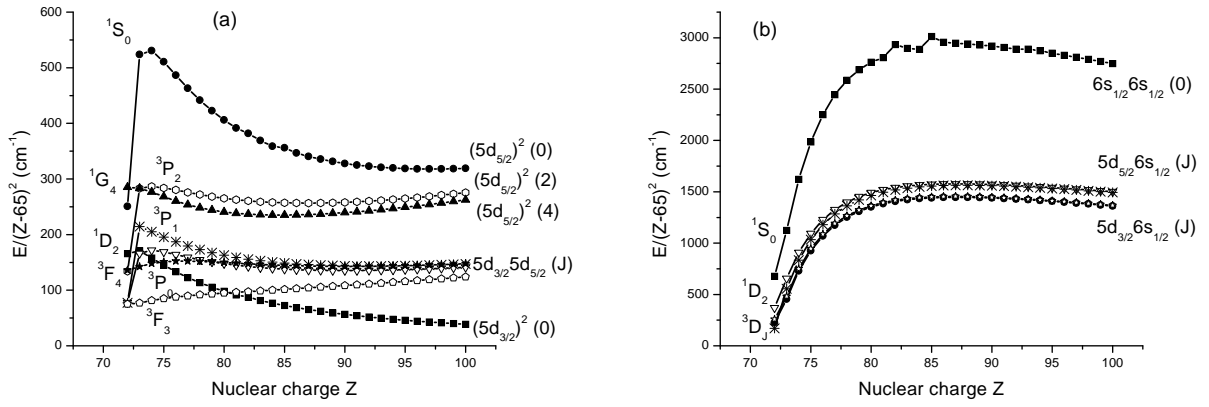


FIG. 2: Z -dependence of the excitation energy $E^{(\text{exc})}/(Z - 65)^2$ in cm^{-1} , for even-parity levels.

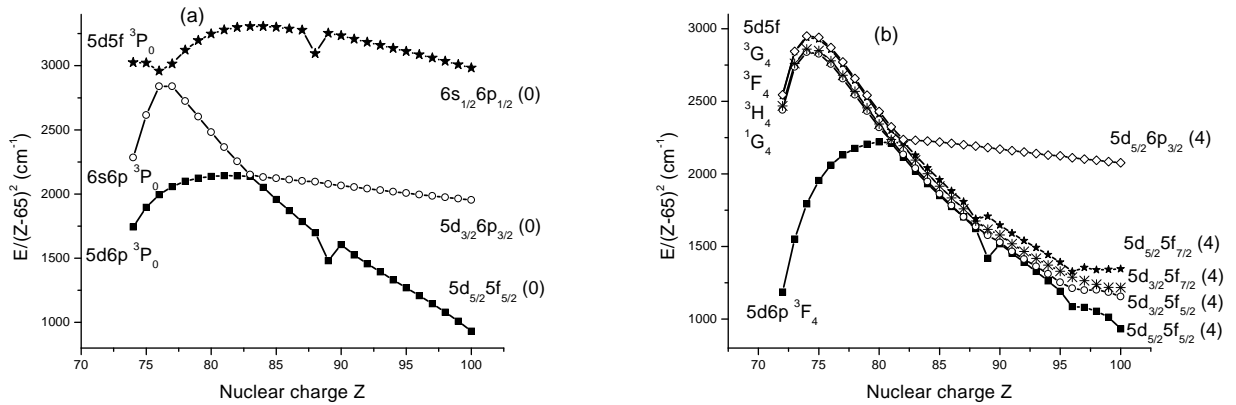


FIG. 3: Z -dependence of the excitation energy $E^{(\text{exc})}/(Z - 65)^2$ in cm^{-1} , for odd-parity levels.

TABLE IV: Uncoupled reduced matrix elements in length L and velocity V forms for even-odd parity transitions in Re^{+5} .

even-parity	odd-parity	$Z_L^{(1)}$	$Z_V^{(1)}$	$Z_L^{(2)}$	$Z_V^{(2)}$	$B_L^{(2)}$	$B_V^{(2)}$	$P_L^{(\text{deriv})}$	$P_V^{(\text{deriv})}$
$5d_{3/2}5d_{3/2}(0)$	$5d_{3/2}6p_{1/2}(1)$	0.84736	0.73795	-0.18176	-0.32201	0.00105	0.00032	0.84733	-0.00001
$5d_{3/2}5d_{3/2}(0)$	$5d_{3/2}6p_{3/2}(1)$	-0.33505	-0.29206	0.00633	0.03976	-0.00074	-0.00053	-0.33502	0.00003
$5d_{3/2}5d_{3/2}(0)$	$5d_{5/2}6p_{3/2}(1)$	0.00000	0.00000	-0.06416	-0.09997	0.00002	0.00000	0.00000	0.00000
$5d_{5/2}5d_{5/2}(0)$	$5d_{3/2}6p_{1/2}(1)$	0.00000	0.00000	-0.04075	-0.08423	-0.00001	-0.00002	0.00000	0.00000
$5d_{5/2}5d_{5/2}(0)$	$5d_{3/2}6p_{3/2}(1)$	0.00000	0.00000	0.05057	0.07583	0.00000	0.00001	0.00000	0.00000
$5d_{5/2}5d_{5/2}(0)$	$5d_{5/2}6p_{3/2}(1)$	0.87030	0.75077	-0.15075	-0.26297	0.00100	0.00055	0.87028	0.00003
$6s_{1/2}6s_{1/2}(0)$	$5d_{3/2}6p_{1/2}(1)$	0.00000	0.00000	-0.30143	0.03609	0.00006	0.00004	0.00000	0.00000
$6s_{1/2}6s_{1/2}(0)$	$5d_{3/2}6p_{3/2}(1)$	0.00000	0.00000	0.20141	-0.18719	-0.00003	-0.00001	0.00000	0.00000
$6s_{1/2}6s_{1/2}(0)$	$5d_{5/2}6p_{3/2}(1)$	0.00000	0.00000	-0.53534	0.90941	0.00006	0.00011	0.00000	0.00000

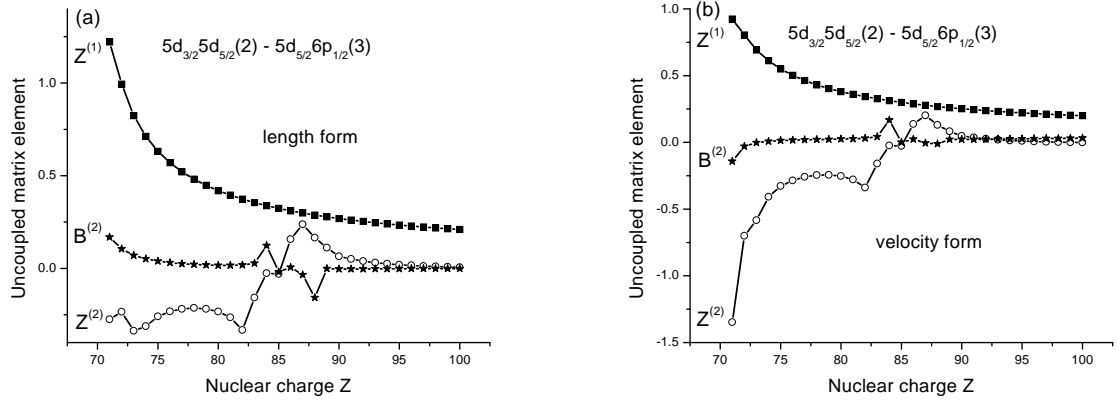
FIG. 4: Uncoupled matrix elements for $5d_{3/2}5d_{5/2}(2)-5d_{5/2}6p_{1/2}(3)$ calculated in velocity and length forms

TABLE V: Line strengths in length L and velocity V forms for even-odd-parity transitions in Re^{+5} .

Level	Level	RMBPT		First order	
		L	V	L	V
$5d^2\ ^3P_0$	$5d6p\ ^3D_1$	0.2632	0.2312	0.4952	0.3749
$5d^2\ ^3P_0$	$5d6p\ ^3P_1$	0.2424	0.2277	0.2673	0.2027
$5d^2\ ^3P_0$	$5d6p\ ^1P_1$	0.0645	0.0651	0.0532	0.0391
$5d^2\ ^1S_0$	$5d6p\ ^3D_1$	0.0040	0.0032	0.0375	0.0288
$5d^2\ ^1S_0$	$5d6p\ ^3P_1$	0.0050	0.0052	0.0272	0.0208
$5d^2\ ^1S_0$	$5d6p\ ^1P_1$	0.3261	0.3437	0.7024	0.5236
$5d^2\ ^3P_1$	$5d6p\ ^3P_0$	0.5035	0.5010	0.5657	0.4208
$5d6s\ ^3D_1$	$5d6p\ ^3P_0$	1.1657	1.1792	1.6949	1.5356
$5d^2\ ^3P_1$	$5d6p\ ^3D_1$	0.0080	0.0081	0.0242	0.0179
$5d^2\ ^3P_1$	$5d6p\ ^3P_1$	0.4143	0.4127	0.5065	0.3774
$5d^2\ ^3P_1$	$5d6p\ ^1P_1$	0.0358	0.0340	0.0346	0.0264
$5d6s\ ^3D_1$	$5d6p\ ^3P_1$	2.1855	2.2762	3.0478	2.7590
$5d^2\ ^3P_1$	$5d6p\ ^1D_2$	0.0274	0.0296	0.0709	0.0528
$5d^2\ ^3P_1$	$5d6p\ ^3P_2$	0.2803	0.2573	0.2959	0.2251
$5d^2\ ^3F_2$	$5d6p\ ^3P_1$	0.1648	0.1639	0.1486	0.1122
$5d^2\ ^3F_2$	$5d6p\ ^3D_2$	0.1145	0.1145	0.1690	0.1262
$5d6s\ ^3D_2$	$5d6p\ ^3P_2$	1.2140	1.2595	1.5450	1.3925
$5d^2\ ^1D_2$	$5d6p\ ^3F_3$	0.0380	0.0361	0.1735	0.1284
$5d6s\ ^3D_2$	$5d6p\ ^3F_3$	2.4488	2.7097	3.3267	3.0271
$5d^2\ ^3F_3$	$5d6p\ ^1D_2$	1.6146	1.6111	1.7279	1.2837
$5d^2\ ^3F_3$	$5d6p\ ^3P_2$	0.1384	0.1440	0.1441	0.1079
$5d6s\ ^3D_3$	$5d6p\ ^3F_2$	0.0020	0.0027	0.0026	0.0024
$5d6s\ ^3D_3$	$5d6p\ ^3P_2$	2.7197	2.9674	3.8172	3.4676
$5d^2\ ^3F_3$	$5d6p\ ^3F_3$	1.6878	1.5330	1.9319	1.4599
$5d^2\ ^3F_3$	$5d6p\ ^3D_3$	0.0528	0.0563	0.0308	0.0219
$5d6s\ ^3D_3$	$5d6p\ ^1F_3$	1.7322	1.8326	2.3084	2.0843
$5d^2\ ^3F_3$	$5d6p\ ^3F_4$	0.1367	0.1294	0.1291	0.0983
$5d6s\ ^3D_3$	$5d6p\ ^3F_4$	11.1345	11.5018	15.2305	13.8004
$5d^2\ ^3F_4$	$5d6p\ ^3F_3$	0.5896	0.5200	0.8001	0.6090
$5d^2\ ^3F_4$	$5d6p\ ^3D_3$	3.6963	3.6447	4.0769	3.0379
$5d^2\ ^3F_4$	$5d6p\ ^1F_3$	0.1442	0.1561	0.1513	0.1095
$5d^2\ ^1G_4$	$5d6p\ ^3D_3$	0.3118	0.3027	0.3497	0.2616
$5d^2\ ^1G_4$	$5d6p\ ^1F_3$	5.6434	5.5815	6.2102	4.6443
$5d^2\ ^3F_4$	$5d6p\ ^3F_4$	1.9537	1.9011	1.9296	1.4447
$5d^2\ ^1G_4$	$5d6p\ ^3F_4$	0.1544	0.1571	0.1535	0.1114

trends of line strengths, oscillator strengths, and transition rates.

A. Transition energies

In Table VI, transition energies are compared with recent measurements [1, 2, 3, 4, 5, 6, 7]. We obtain good agreement with the experiment for low-lying $5d^2$, $5d6s$, and $5d6p$ levels. We also we obtain reasonable agreement (500 - 1000 cm^{-1}) for highly-excited $5d5f$ levels in Re VI, Os VII, and Ir VIII ions. However, we disagree substantially (2000 - 10000 cm^{-1}) for $5d5f$ levels in Pt IX, Au X, and Hg XI ions. As mentioned in Refs. [4, 5, 6], mixing between levels of the $5d5f$ configuration and the core excited configurations with a $5p$ hole could be very important for Pt IX, Au X, and Hg XI ions. Indeed, sub-

stantial mixing of the $5p^55d^3$ and $5p^65d5f$ configurations was found in Ref. [6]. From this, we conclude that the present values for $5d5f$ configurations in Pt IX, Au X, and Hg XI are less reliable ($\sim 1\%$) than data for Re VI, Os VII, and Ir VIII.

B. Fine structure of the $5d6p$ triplets

The fine-structure intervals for the 3P , 3D , and 3F terms of $5d6p$ configuration divided by $(Z - 65)^2$ are shown in Fig. 5. The fine structures of these levels do not follow the Landé rules even for small Z ; the 3P levels are partially inverted, while the 3D and 3F levels show regular ordering of the fine-structure splittings for both low and high Z . The unusual splittings are caused by changes from LS to jj coupling and by mixing from other triplet and singlet states. Comparisons are made with experimental data from [1, 2, 3, 4, 5, 6, 7] in Fig. 5. Excellent agreement (0.3% - 3%) is found for the four intervals 3P_1 - 3P_0 , 3D_3 - 3D_2 , 3F_4 - 3F_3 , and 3F_3 - 3F_2 . The agreement decreases for the 3P_2 - 3P_1 and 3D_2 - 3D_1 intervals, from 10% for Re^{+5} to 2% for Hg^{+10} . Experimental energies for other ions would be very helpful in confirming the Z dependence shown in Fig. 5.

C. Line strengths and oscillator strengths in Yb-like ions

Trends of the Z dependence of line strengths and oscillator strengths, are shown in Figs. 6 and 7. In Fig. 6, we illustrate the Z dependence of line strengths for the four $5d^2$ - $5d6p$ transitions calculated (a) by RMBPT and (b) in first-order to illustrate once again the importance of including second-order matrix elements. Comparing the curves in Fig. 6a and Fig. 6b, we can see that the Z dependence is the same for both cases except for the small region $Z = 80$ - 88 . The singularities in this region are already present for uncoupled dipole matrix elements. The second-order contribution for the $5d_{3/2}5d_{5/2}(2)$ - $5d_{5/2}6p_{1/2}(3)$ uncoupled matrix element is shown in Fig. 4. Similar singularities appeared for other uncoupled matrix elements between even-parity $J=2$ states and odd-parity $J=3$ states. Consequently, those singularities also appear in the coupled matrix elements and the line strengths shown in Fig. 6.

The Z dependence is more complicated for transitions between even-parity states with $J=1$ and odd-parity states with $J=0$, as seen in Fig. 7, where we give oscillator strengths for four transitions calculated (a) by RMBPT and (b) in first-order. The oscillator strength curves are not smooth functions of Z , even in first-order. The singularities shown in the four curves of Fig. 7b arise from the strong mixing between three states of the odd-parity complex with $J=0$. The mixing of $5d_{5/2}5d_{5/2}$, $5d_{3/2}6p_{3/2}$, and $6s_{1/2}6p_{1/2}$ states was discussed earlier in Fig. 3a where it was shown that avoided crossings occur

TABLE VI: Energy levels (cm^{-1}) in ytterbium isoelectronic sequence. Comparison of RMBPT results with experimental data presented in Refs. [1, 2, 3, 4, 5].

Level	Re VI		Os VII		Ir VIII		Pt IX		Au X		Hg XI	
	RMBPT	[1]	RMBPT	[2, 3]	RMBPT	[2, 3]	RMBPT	[4]	RMBPT	[5]	RMBPT	[5]
$5d^2\ ^3F_2$	0	0	0	0	0	0	0	0	0	0	0	0
$5d^2\ ^3F_3$	8491	8167	10604	10308	12932	12672	15490	15250	18284	18077	21325	21175
$5d^2\ ^3P_0$	14495	14379	16117	15837	17670	17254	19174	18612	20638	19949	22055	21255
$5d^2\ ^3F_4$	15095	14679	18409	18049	21920	21615	25633	25359	29550	29309	33677	33481
$5d^2\ ^1D_2$	16866	16577	19852	19444	22905	22436	26146	25568	29568	28925	33211	32513
$5d^2\ ^3P_1$	19556	19142	22624	22098	25841	25222	29238	28515	32832	32039	36643	35802
$5d^2\ ^1G_4$	26807	26657	31496	31274	36522	36253	41949	41610	47818	47451	54165	53918
$5d^2\ ^3P_2$	28371	27723	33932	33127	39735	38878	45962	44991	52588	51566	59691	58835
$5d^2\ ^1S_0$	51056	50492	58851	57710	66656	65022	74624	72527	82848	80385	91380	88897
$5d6s\ ^3D_1$	92656	92312	129438	129244	169138	169223	211579		256622		304159	
$5d6s\ ^3D_2$	94554	94262	131488	131416	171413	171485	214009		259236		306918	
$5d6s\ ^1D_2$	109374	108709	148595	148023	191018	190553	236412		284633		335596	
$5d6s\ ^3D_3$	103444	102712	142679	142163	185041	184748	230364		278518		329409	
$6s^2\ ^1S_0$	198652		272504	282345	352159	363633	437184		527172		621600	
$5d6p\ ^3F_2$	163618	162134	209906	208659	259044	258017	310888	310064	365322	364711	422250	422506
$5d6p\ ^3D_1$	166538	166077	213084	212862	262439	262461	314456	314751	369016	369624	426038	426672
$5d6p\ ^3D_2$	176168	174761	224886	223453	276670	275872	331369	330850	388865	388660	449056	449335
$5d6p\ ^3F_3$	177212	175502	226212	224741	278237	276994	333148	332117	390829	390038	451183	450786
$5d6p\ ^1D_2$	182853	181154	233874	232453	288280	287122	345942	345026	406770	406109	470688	470408
$5d6p\ ^3D_3$	186672	185022	238186	236726	293068	291792	351186	350075	412435	411533	476719	476134
$5d6p\ ^3P_1$	187037	185963	238656	237682	293545	292734	351634	350986	412843	412413	477109	476749
$5d6p\ ^3P_0$	189199	187780	241043	239794	296204	295142	354580	353689	416091		480682	480075
$5d6p\ ^3F_4$	195446	193260	249334	247354	306792	305005	367714	366087	432023	430576	499662	498310
$5d6p\ ^3P_2$	196486	194539	250142	248453	307362	305894	368050	366803	432129	431126	499533	498771
$5d6p\ ^1F_3$	197742	195691	251254	249401	308315	306697	368814	367435	432644	431579	499643	499109
$5d6p\ ^1P_1$	200506	200437	255391	255246	313586	313520	375052	375145	439684	440120	507190	508193
$6s6p\ ^3P_0$	261637		343490		408884		460493	456143	510225		558566	
$6s6p\ ^3P_1$	265550		341677	341844	394150	391888	443224	438038	490445		536100	
$6s6p\ ^3P_2$	281644	279156	333322	332501	381777	379116	428519	424403	473776		517742	
$5d5f\ ^1G_4$	282611	280575	333410	331454	382478	380334	430103	425349	476544		522022	
$5d5f\ ^3F_2$	282986	281906	341072	340330	391578	388229	440422	435302	487930		534343	
$5d5f\ ^3F_3$	283375	283559	334390	334240	383305	380724	430253	422093	475351		518717	
$5d5f\ ^3H_4$	284803	282853	336142	334302	385817	383508	434072	430412	481126		527163	
$5d5f\ ^3G_3$	286237	286426	338249	337436	388358	385282	436878	425627	484128		530397	
$5d5f\ ^3H_5$	287360	285346	339706	337535	390378	387545	439680	436230	487868		535150	
$5d5f\ ^3D_1$	289100	290208	349008		408218	406542	459678	456053	509418		557828	
$5d5f\ ^1D_2$	289565	288853	348392	347386	399983	397557	449925	442048	498451		545750	
$5d5f\ ^3F_4$	292767	290824	345648	343897	396931	393669	446783	439406	495294		542569	
$5d5f\ ^3G_4$	294002	293741	347287	346144	398865	396001	449051	445365	498219		546694	
$5d5f\ ^3D_2$	295265	294688	354838	354012	408411	405867	460122	456798	510546		559987	
$6s6p\ ^1P_1$	295457		357819	356849	420585	421774	477574		532630		586680	
$5d5f\ ^3D_3$	295676	295836	349683	349155	401804	397003	452259	436157	501264		549026	
$5d5f\ ^3G_5$	295717	295928	349829	349324	402320	399128	453392	443691	503255		552106	
$5d5f\ ^3H_6$	296143	292600	349940		402394		453792		504385		554394	
$5d5f\ ^1F_3$	300071	300794	356198	356322	410808	408418	464085	461735	516269		567655	
$5d5f\ ^3P_2$	301078	301178	371823		465428		565480		671378		782904	
$5d5f\ ^3P_1$	301570	302600	362544	363927	440737		534533		634090		738793	
$5d5f\ ^3P_0$	302331	303600	358117	356587	434121		527597		626622		730708	
$5d5f\ ^1H_5$	303559	307440	361850	364949	418559	420291	473757	470214	527612		580323	
$5d5f\ ^1P_2$	317422	317600	396700		489065		589085		695429		807602	

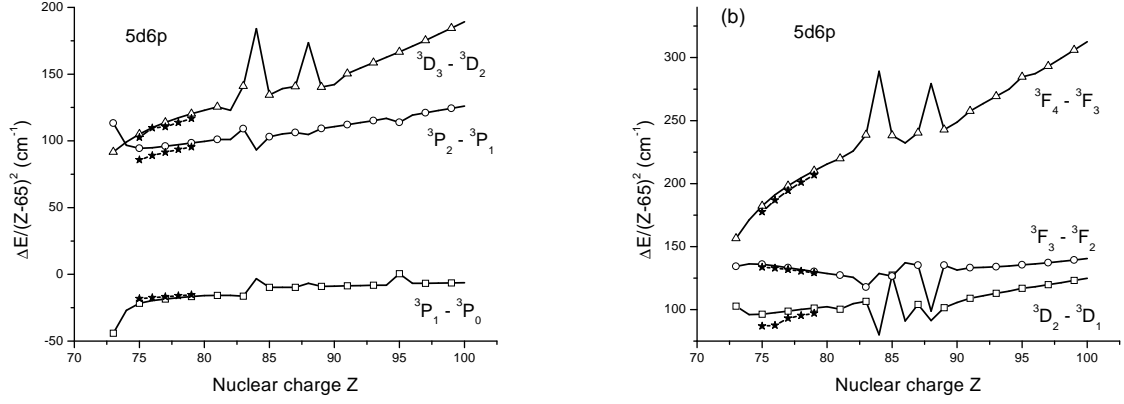


FIG. 5: Fins-structure intervals $\Delta E/(Z-65)^2$ in cm^{-1} of $5d6p\ ^3P$, $5d6p\ ^3D$, and $5d6p\ ^3F$ terms as function of Z . Experimental data represented by the * symbol are from [1, 2, 3, 4, 5, 6, 7]

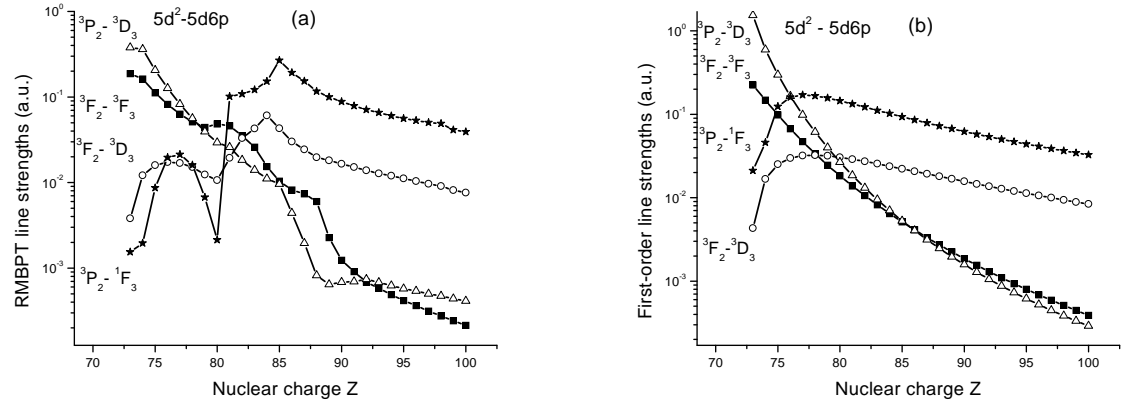


FIG. 6: Line strengths for $5d^2 - 5d6p$ transitions in Yb-like ions: (a) - RMBPT, (b) - First-order approximation.

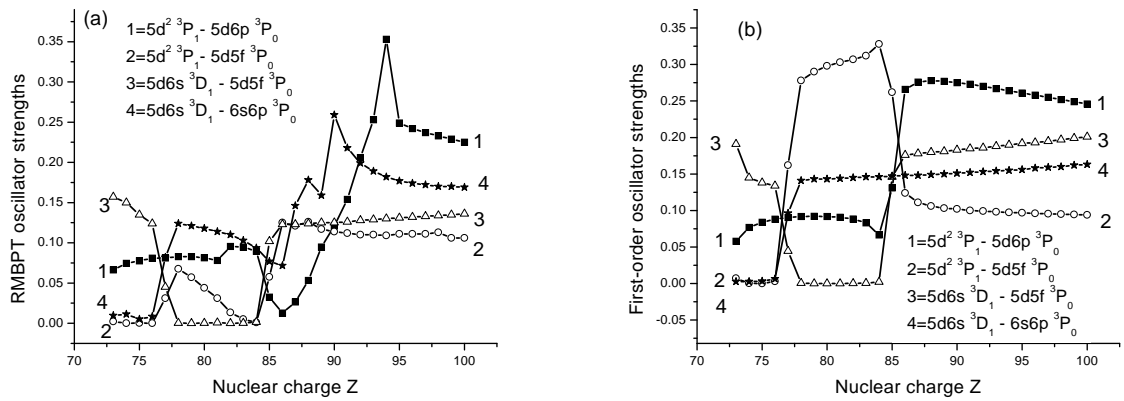


FIG. 7: Oscillator strengths for transitions from even-parity complex with $J=1$ to odd-parity complex with $J=0$ in Yb-like ions: (a) - RMBPT, (b) - First-order approximation.

near $Z=76$ and 84 .

IV. CONCLUSION

In summary, a systematic second-order RMBPT study of the energies of the $5d^2$, $5d6s$, $6s^2$, $5d6p$, $5d5f$, and $6s6p$ states of Yb-like ions has been presented. These calculations agree with existing experimental energy data for intermediate $Z=75$ to 80 at the level of $500\text{-}1000\text{ cm}^{-1}$ for low-lying $5d^2$, $5d6s$, and $5d6p$ levels. They provide a smooth theoretical reference database for the identification of lines.

Also presented is a systematic second-order relativistic RMBPT study of reduced matrix elements, line strengths, oscillator strengths, and transition rates for allowed and forbidden electric-dipole transitions in Yb-like ions with nuclear charges ranging from $Z = 72$ to 100 . The dipole matrix elements include retardation and correlation corrections from Coulomb and Breit interactions. Both length and velocity forms of the matrix elements are evaluated, and $\sim 5\%$ differences, caused by the non-locality of the starting DF potential, are found between the two forms.

We believe that our results will be useful in analyzing existing experimental data and planning new experiments. There remains a paucity of experimental data for many of the higher ionized members of this sequence, both for term energies and for transition probabilities and lifetimes. Additionally, matrix elements from the present calculations will provide basic theoretical input for calculations of reduced matrix elements, oscillator strengths, and transition rates in three-electron Lu-like ions.

Acknowledgments

The work of W.R.J. and M.S.S. was supported in part by National Science Foundation Grant No. PHY-01-39928. U.I.S. acknowledges partial support by Grant No. B503968 from Lawrence Livermore National Laboratory. The work of J.R.A was performed under the auspices of the U. S. Department of Energy by the University of California, Lawrence Livermore National Laboratory under contract No. W-7405-Eng-48. We also acknowledge helpful discussions with Professor A.N. Ryabtsev.

APPENDIX A: THE SECOND-ORDER DOUBLE-EXCITATION CONTRIBUTION

Here, we consider the second-order double-excitation contribution to explain singularities in the Z dependence of energy levels given in Figs. 2 and 3. A typical contribution from one of the double-excitation diagram for the

second-order interaction energy has the form [11]

$$A_l(vw; v'w') \propto \sum_{mn} \sum_{kk'} \frac{X_k(vwmn)X_{k'}(mnv'w')}{\epsilon_{v'} + \epsilon_{w'} - \epsilon_m - \epsilon_n}, \quad (\text{A1})$$

where $X_{k'}(vwmn)$ are products of angular coupling coefficients and Slater integrals [11], ϵ_m is the single-particle energy for state m , and v designates a single-particle valence state $(n_v l_v j_v)$. For the case of a $[\text{Xe}]4f^{14}$ core, sums over m and n include $5d_{3/2}$, $5d_{5/2}$, $5f_{5/2}$, $5f_{7/2}$, $5g_{7/2}$, $5g_{9/2}$, and all states with principal quantum number $n > 5$. We must, however, exclude terms with pairs (mn) that are included in model space. Therefore, we remove the pairs $(5d5d)$, $(5d6s)$, and $(6s6s)$ since they are in the even-parity model space and pairs $(5d6p)$, $(5d5f)$, and $(6s6p)$ in the odd-parity model space.

As an example, let us consider the singularity near $Z=85$ in the curve describing the energy of the $6s^2$ level in Fig. 2b. The denominator in Eq. (A1) is $D = 2\epsilon_{6s} - \epsilon_m - \epsilon_n$ for the matrix element $A_l(6s_{1/2}6s_{1/2}; 6s_{1/2}6s_{1/2})$. For an ion with $Z=85$, D becomes very small when $(mn)=(5d_{3/2}6d_{3/2})$ since $\epsilon_{6s_{1/2}} = -9.488404$ a.u., $\epsilon_{5d_{3/2}} = -12.069226$ a.u., and $\epsilon_{6d_{3/2}} = -6.932272$ a.u., giving $D=0.02469$. This one term dominates the matrix element $A_l(6s_{1/2}6s_{1/2}; 6s_{1/2}6s_{1/2})$ and increases its size by a factor of six in comparison with values for neighboring Z , explaining the singularity at $Z=85$ in Fig. 2b. The explanation of the sharp features in the curves describing energies of the $6s_{1/2}6p_{1/2}$ and $5d_{5/2}5f_{5/2}$ levels in Fig. 3 is similar.

APPENDIX B: THE SECOND-ORDER DIPOLE MATRIX ELEMENT

A typical contribution from one of the second-order correlation corrections to the dipole matrix element $(vw(J) - v'w'(J'))$ has the form [13]

$$Z^{(\text{corr})}[vw(J) - v'w'(J')] \propto \sum_i \frac{Z_{iv}X_k(v'w'wi)}{\epsilon_i + \epsilon_w - \epsilon_{v'} - \epsilon_{w'}},$$

where Z_{iv} is a single-electron dipole matrix element. In the sum over i , only terms with vanishing denominators are excluded. For the $5d_{5/2}5d_{3/2}(2) - 5d_{5/2}6p_{1/2}(3)$ transition, we obtain

$$\begin{aligned} & Z^{(\text{corr})}[5d_{5/2}5d_{3/2}(2) - 5d_{5/2}6p_{1/2}(1)] \\ & \propto \sum_i \frac{Z(i, 5d_{5/2})X_k(5d_{5/2}6p_{1/2} 5d_{3/2}i)}{\epsilon_i + \epsilon(5d_{3/2}) - \epsilon(5d_{5/2}) - \epsilon(6p_{1/2})}. \end{aligned}$$

For the case $i=5f_{7/2}$ and $Z=84$, the denominator becomes

$$\epsilon_i + \epsilon(5d_{3/2}) - \epsilon(5d_{5/2}) - \epsilon(6p_{1/2}) = 0.003.$$

This one term dominates the entire matrix element. For the $5d_{5/2}5d_{5/2}(0) - 5d_{3/2}6p_{1/2}(1)$ transition, the denominator becomes very small at $Z=88$ when $i=5f_{7/2}$.

$$\epsilon_i + \epsilon(5d_{5/2}) - \epsilon(5d_{3/2}) - \epsilon(6p_{1/2}) = -0.056.$$

Again, this single term dominates the matrix element.

A typical contributions from the second-order RPA correction for dipole matrix element ($vw(J) - v'w'(J')$) has the form

$$Z_1^{(\text{RPA})}[vw(J) - v'w'(J')] \propto \sum_i \frac{Z_{nb}X_k(wnv'b)}{\epsilon_n + \epsilon_w - \epsilon_{v'} - \epsilon_b},$$

where the index b designates core states and n designates an excited state. For the special case of the $5d_{5/2}5d_{3/2}[2] - 6p_{1/2}5d_{5/2}[1]$ transition, we obtain

$$Z_1^{(\text{RPA})}[5d_{3/2}5d_{5/2}(2) - 6p_{1/2}5d_{5/2}(3)]$$

$$\propto \sum_n \sum_b \frac{Z(b,n)X_k(5d_{3/2}b 6p_{1/2}n)}{\epsilon_n + \epsilon(5d_{3/2}) - \epsilon(6p_{1/2}) - \epsilon_b}.$$

In the case of $b=5p_{3/2}$ and $n=5d_{3/2}$ for nuclear charge $Z=88$, the denominator becomes

$$\epsilon(5d_{3/2}) + \epsilon(5d_{3/2}) - \epsilon(6p_{1/2}) - \epsilon(5p_{3/2}) = -0.278.$$

As before, the small value of the denominator leads to an anomalous increase in the size of the RPA matrix element.

-
- [1] J. Sugar, J.-F. Wyart, G. J. van het Hof, and Y. N. Joshi, *J. Opt. Soc. Am. B* **11**, 2327 (1994).
- [2] G. J. van het Hof, Y. N. Joshi, J.-F. Wyart, and J. Sugar, *J. Res. Natl. Inst. Stand. Technol.* **100**, 687 (1995).
- [3] R. R. Kildiyarova, Y. N. Joshi, and J. Sugar, *Phys. Scr.* **53**, 560 (1996).
- [4] R. R. Kildiyarova, Y. N. Joshi, S. S. Churilov, A. N. Ryabtsev, and J. Sugar, *Phys. Scr.* **55**, 438 (1997).
- [5] S. S. Churilov, R. Gayasov, R. R. Kildiyarova, Y. N. Joshi, and A. N. Ryabtsev, *Phys. Scr.* **57**, 626 (1998).
- [6] S. S. Churilov and Y. N. Joshi, *Phys. Scr.* **58**, 425 (1998).
- [7] V. I. Azarov and S. S. Churilov, *Opt. Spectr.* **88**, 11 (2000).
- [8] R. D. Cowan, *The Theory of Atomic Structure and Spectra* (University of California Press, Berkeley, 1981).
- [9] S. G. Porsev, Y. G. Rakhlina, and M. G. Kozlov, *Phys. Rev. A* **60**, 2781 (1999).
- [10] W. C. Martin, R. Zalubas, and L. Hagan, *Atomic Energy Levels - The Rare-Earth Elements* (U. S. Government Printing Office, Washington DC, 1978).
- [11] M. S. Safronova, W. R. Johnson, and U. I. Safronova, *Phys. Rev. A* **53**, 4036 (1996).
- [12] W. R. Johnson, M. S. Safronova, and M. S. Safronova, *Phys. Scr.* **56**, 252 (1997).
- [13] U. I. Safronova, W. R. Johnson, M. S. Safronova, and A. Derevianko, *Phys. Scr.* **59**, 286 (1999).
- [14] U. I. Safronova, W. R. Johnson, and H. G. Berry, *Phys. Rev. A* **61**, 052503 (2000).
- [15] U. I. Safronova, W. R. Johnson, D. Kato, and S. Ohtani, *Phys. Rev. A* **63**, 032518 (2001).
- [16] P. F. A. Klinkenberg, T. A. M. V. Kleef, and P. E. Noorman, *Physica* **27**, 151 (1962).
- [17] W. R. Johnson, S. A. Blundell, and J. Sapirstein, *Phys. Rev. A* **37**, 2764 (1988).
- [18] M. H. Chen, K. T. Cheng, and W. R. Johnson, *Phys. Rev. A* **47**, 3692 (1993).
- [19] I. Lindgren and J. Morrison, *Atomic Many-Body Theory* (Springer-Verlag, New York, 1986), 2nd ed.
- [20] U. I. Safronova, A. Derevianko, M. S. Safronova, and W. R. Johnson, *J. Phys. B* **32**, 3527 (1999).